Journal of Engineering Research

Volume 7 | Issue 1 Article 7

2023

Pneumatic Artificial Muscles (PAMs) Identification for Actuating a Wrist-Joint Rehabilitation Robot

Omer Omer

Journal of Engineering Research (ERJ)
©Tanta University, Faculty of Engineering
https://erjeng.journals.ekb.eg/
ISSN: 2356-9441
e ISSN: 2735-4873

Pneumatic Artificial Muscles (PAMs) Identification for Actuating a Wrist-Joint Rehabilitation Robot

Omar Mehrez [a,*], Amr M. Hegazy [a], SA El-Agouz [a,b], M.M. Bassuoni [a]

[a] Department of Mechanical Power Engineering, Faculty of Engineering, Tanta University, Egypt
[b] Faculty of Industry and Energy Technology, Delta Technological University, Quesna, Egypt
Email: omar.mehrez@f-eng.tanta.edu.eg

***Abstract*- Pneumatic Artificial Muscles (PAMs) are the most promising type of pneumatic-based actuators. Recently, they have been widely used in medical and rehabilitation robotic systems due to their flexibility, reliability, and high load-to-weight ratio. The aim of this work is to introduce an accurate mathematical model for describing the performance of pneumatic artificial muscles under different applied pressures and loads by examining different previously proposed models. Being motivated by the muscles' usage in a wearable robotic device for wrist rehabilitation where the required muscle force is not so large, it is interesting to consider the model that best expresses the muscle behavior over a lower range of the muscle force. An experimental system for measuring muscle contraction at different applied pressures and loads is set up. Then, an algorithm for the parameters identification of the examined models based on the least squared error approach is developed using MATLAB Software.**

***Keywords*: Pneumatic artificial muscles identification; Wrist-joint rehabilitation robot.**

I. INTRODUCTION

Over the years, actuators are the backbone of researchers' applications like robotics, mechanization, and industrial. The actuators' main types are electrical motors, magnetic, hydraulic, and pneumatic-based ones. The application type and limitations of the system determine the efficient kind. During the last decade, pneumatic actuators have significant increase usage in industrial and medical areas. This use grows because of its advantages, such as high strength, high power-to-weight ratio, and small weight [1, 2].

Pneumatic Muscle Actuators [3] are one of the pneumatic-based types. Originally, they were introduced to help the movement of handicapped patients [4]. They are also known as McKibben Pneumatic Artificial Muscles (PAMs) and fluidic actuators [3-9]. Pure rubber latex was the PAMs material and used a double helical braided shell to protect the PAMs. This shell contract when expanded radially. [10].

Later, the usage of these actuators was extended to more applications such as assisting disabled individuals, service robotics, and even industrial applications replacing the conventional pneumatic actuators due to their high strength [11, 12]. It has many advantages against conventional pneumatic cylinders, such as a high force-to-weight ratio, variable installation possibilities, no movable mechanical parts, lower compressed–air consumption, and low cost [13].

Recently, Orthotic exoskeleton apparatuses and other rehabilitation engineering devices widely depend on PAMs as main actuator [14-16]. Additional usages for PAMS are in biomimetic robotics [17, 18] and the evolution of artificial fine-motion limbs [17, 19].

Most commercial PAMs are consisting of a rubber bladder covered by a helically braided shell, and each end have an appropriate metal fitting attached to it. When compressed air is applied to the interior of the rubber tube, it contracts in length and radially expands, as shown in Fig 1. As the air exits, the muscle operates as a spring for restoring the PAM to its initial shape [20].

The PAM converts the fluid power to mechanical power in the form of a pulling force and a contraction in length. Both the pulling force and contraction length are depending on the applied pressure in addition to the geometrical and physical characteristics of the muscle, which were described by different mathematical models [20-24]. Most of these models are introducing the output force as a function of the applied pressure and contraction with respect to the different characteristics of the muscle.

This work aims to introduce an accurate mathematical model for describing the performance of PAMs under different applied pressures and loads by examining different previously proposed models. Since the muscles will be used as actuators in a wrist rehabilitation robot, see Fig. 2, where the actuation forces are not so large, the muscles are modeled at a low force range. Firstly, an experimental system for measuring the contraction of the muscle under different applied pressures and loads is set up. After that, different mathematical models are evaluated for describing the experimental data. An algorithm is developed using MATLAB Software to identify the parameters of each model.

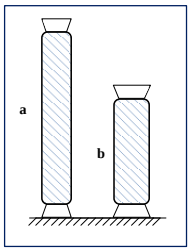

Fig. 1 Operation of the pneumatic artificial muscle a) initial state b) pressurized state.

DOI: 10.21608/ERJENG.2023.179380.1131

Journal of Engineering Research (ERJ)
©Tanta University, Faculty of Engineering
https://erjeng.journals.ekb.eg/
ISSN: 2356-9441
e ISSN: 2735-4873

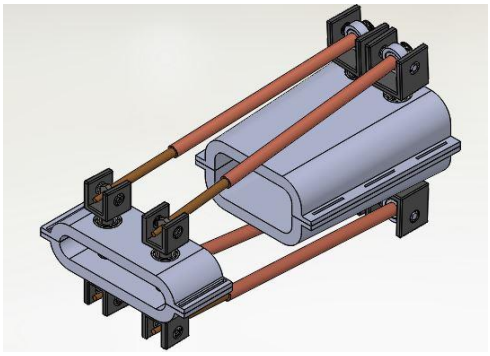

Fig. 2 Schematic diagram of a wrist-joint rehabilitation robot.

The paper is organized as follows: in section I the experimental set-up of the system is introduced. Different mathematical models for PAMs and the developed algorithm for the identification of the model parameters are discussed in section II. Section III deals with the discussion of the results. Conclusions and future work are given in section IV.

II. EXPERIMENTAL SET-UP

Figs. 3 and 4 show the corresponding schematic diagram of the system and the experimental set-up, respectively for measuring the muscle contraction at every applied pressure and tensile load. The experimental system includes the PAM, control devices, and measuring instruments. An air compressor of 0:8bar pressure range and 25L capacity with a 2HP driving motor represents the source of the pressurized air to the muscle. A service unit with a pressure regulator (AC4010-04) is equipped to filter and lubricate the output air from the compressor, then regulate it to the required pressure. After that, the air is directed to the muscle.

The PAM has one port for the inlet and outlet of the air pressure. It's fixed at one end, while the other end is connected to the load via a belt-pully mechanism. A linear encoder (K+C-S5-D-59192) is attached to the movable end of the muscle, in between the load and the muscle, to measure the muscle displacement once the air pressure is applied at a certain load. The linear encoder has a range of 200mm, a resolution of 5µm, and an accuracy of ±40µm. The displacement of the PAM is displayed on the data logger with the linear encoder.

For each value of the applied pressure (from 1:7 bar with a step of 1 bar), the load is changed from 0:30 kg. Then the measured displacement is used to calculate the contraction of the muscle. The muscle contraction is the ratio between the differential value of the nominal length with the displacement and the nominal length of the muscle, which is illustrated later.

The applied pressure to the muscle is measured at the entrance by a pressure transducer (MAN-LD3S6B7S) powered by a 24V power supply. It has a range of 0:10 bar, an accuracy of ±1% of full scale, and a sensitivity of ±1%.

Figure 5 shows the technical specification of the used PAM. The muscle model is (DMSP-10-230N-AM-CM) manufactured by Festo Co. It has an inner diameter of 10mm and a nominal length of 230mm at 0N load and 0bar gauge pressure. The maximum contraction is 25% of the nominal length at a max pressure of 8 bar gauge pressure and 0N load. The maximum permissible force is 630N.

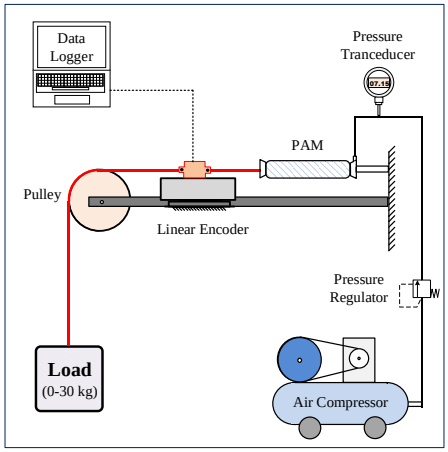

Fig. 3 Schematic diagram of the experimental set-up.

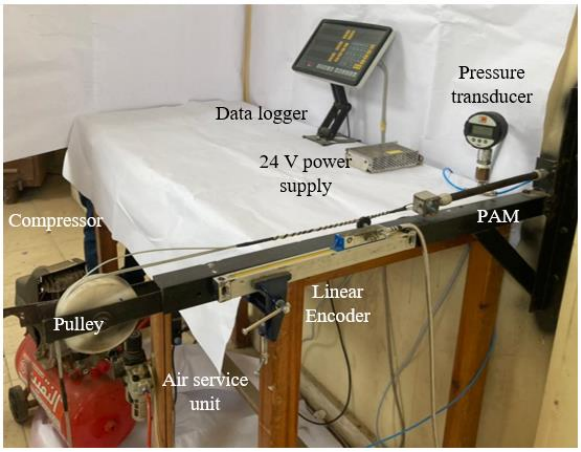

Fig. 4 The experimental set-up.

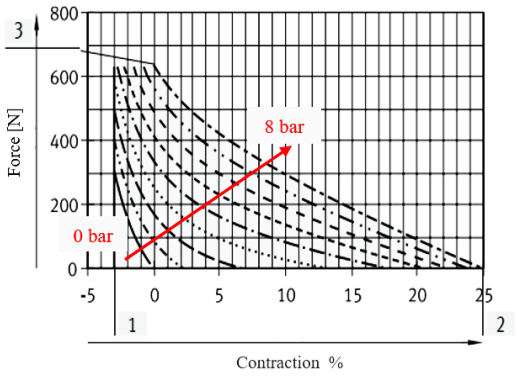

Fig. 5 PAM force against pressure and contraction for (DMSP-10-230N-AM-CM) [25].

DOI: 10.21608/ERJENG.2023.179380.1131

Journal of Engineering Research (ERJ)
©Tanta University, Faculty of Engineering
https://erjeng.journals.ekb.eg/
ISSN: 2356-9441
e ISSN: 2735-4873

The experimental procedure is done as follows for each applied pressure to the muscle:

- The regulated air from the compressor is directed to the muscle and measured by the pressure transducer.
- The muscle is firstly zero-loaded. Then, the muscle displacement is measured by the linear encoder, and hence the contraction is calculated.
- The load is gradually increased by a 2.5kg step, and in each case, the corresponding displacement is measured and hence the contraction is calculated.

This procedure is repeated for 3times for each applied pressure, and after that, the measured data are averaged.

III. MATHEMATICAL MODELING

In recent years, PAMs mathematical modeling has had plenty of attention from researchers to use in their works due to its growing usage. The relation describing the applied pressure and the corresponding contraction of the muscle to the axial force is the aim of each model. There are many parameters that decide the model of the PAMs like pulling force upon the applied pressure and the corresponding contraction, muscle diameter, and material properties. The PAMs models are a function of these variables due to their major role in the PAMs behavior [20, 21, 26-28].

For utilizing the PAM as a linear actuator to handle tension force, one end of the muscle should be attached to an external load, and the other end is fixed. As noted, the muscle's geometrical properties and physical operations inside the muscle act as the base for describing efficient mathematical model relating PAM variables. The relation between the applied pressure, muscle force, volume, and the corresponding contraction is the major characteristic of PAMS.

The original methods of modeling were based on the geometry of the muscle. Chou and Hannaford [21] and Tondu and Lopez [20] are the most common models in geometrical models.

In Chou and Hannaford's model, the muscle can be modeled as a cylinder under some assumptions, see Fig. 6, with a muscle length L, thread length b, turns number n, and inner diameter D. The angle θ is the angle of the threads with the longitudinal axis [21, 29].

Thread length b and its turns number n are geometrical constants of the muscle assuming non-expansion braiding fibers. Inner diameter D and muscle length L are modeled as a function of the initial angle θ as follows:

$$L = b\cos\theta \tag{1}$$

$$D = b\frac{\sin\theta}{n\pi} \tag{2}$$

Utilizing the energy conservation principle, the PAM force F can be estimated upon the applied gauge pressure P multiplied by the volume change concerning length as:

$$F(L,P) = \frac{Pb^2\left[3\frac{L^2}{b^2} - 1\right]}{4\pi n^2} \tag{3}$$

Another simple geometrical model of PAM is that of Tondu and Lopez [20]. Researchers depended on the theory of virtual work to conclude the mathematical model approach.

$$F(\varepsilon,P) = \left(\frac{\pi}{4}D^2\right)P[h(1-\varepsilon)^2 - y] \tag{4}$$

where ε is the contraction given as:

$$\varepsilon = \frac{L_o - L}{L_o} \tag{5}$$

and h and y are defined as:

$$h = \frac{3}{\tan^2\theta} \tag{6}$$

$$y = \frac{1}{\sin^2\theta} \tag{7}$$

Eqn. (4) was modified by both Tondu and Lopez in [20] and Kerscher et al. in [28] with correction factors K and μ:

$$F(\varepsilon,P) = \left(\frac{\pi}{4}D^2\right)P[a(1-k\varepsilon)^2 - b] \tag{8}$$

$$F(\varepsilon,P) = \mu\left(\frac{\pi}{4}D^2\right)P[a(1-k\varepsilon)^2 - b] \tag{9}$$

Where:

$$k = a_k e^{-P} - b_k \tag{10}$$

$$\mu = a_\varepsilon e^{-40.\varepsilon} - b_\varepsilon \tag{11}$$

Marked differences between the experimental and theoretical results using Eqns. (8) and (9) clarified in [30, 31]. To eliminate these differences, J. Sarosi et al. introduced a new approximation algorithm with six constant parameters for the force generated by fluidic muscles in terms of only the muscle pressure P and contraction ε [22, 32], given as:

$$F(\varepsilon,p) = (a.p + b).e^{c.\varepsilon} + d.p.\varepsilon + e.p + f \tag{12}$$

where a, b, c, d, e, and f are constants.

For the modeling of the considered muscle, the five approaches, given in Eqns. (3), (4), (8), (9), and (12), have been applied to get a relation of the muscle force with the corresponding contraction at certain applied pressure. Experimental data are used to identify the constants in each relation. The relation gives the least error between the calculated and measured forces are considered the model for the muscle.

The algorithm used in the identification of each model parameters is developed using MATLAB software. Fig. 7 shows the flowchart of the algorithm. The steps of running the algorithm are discussed below based on Eqn. (12). They are applied for each model with slight changes according to the relation of each one.

DOI: 10.21608/ERJENG.2023.179380.1131

Journal of Engineering Research (ERJ)
©Tanta University, Faculty of Engineering
https://erjeng.journals.ekb.eg/
ISSN: 2356-9441
e ISSN: 2735-4873

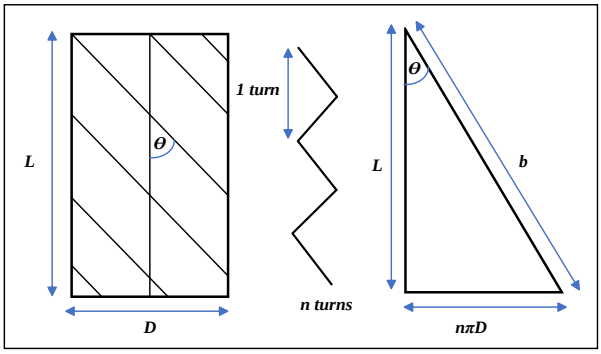

Fig. 6 Parameters of the pneumatic artificial muscle [21].

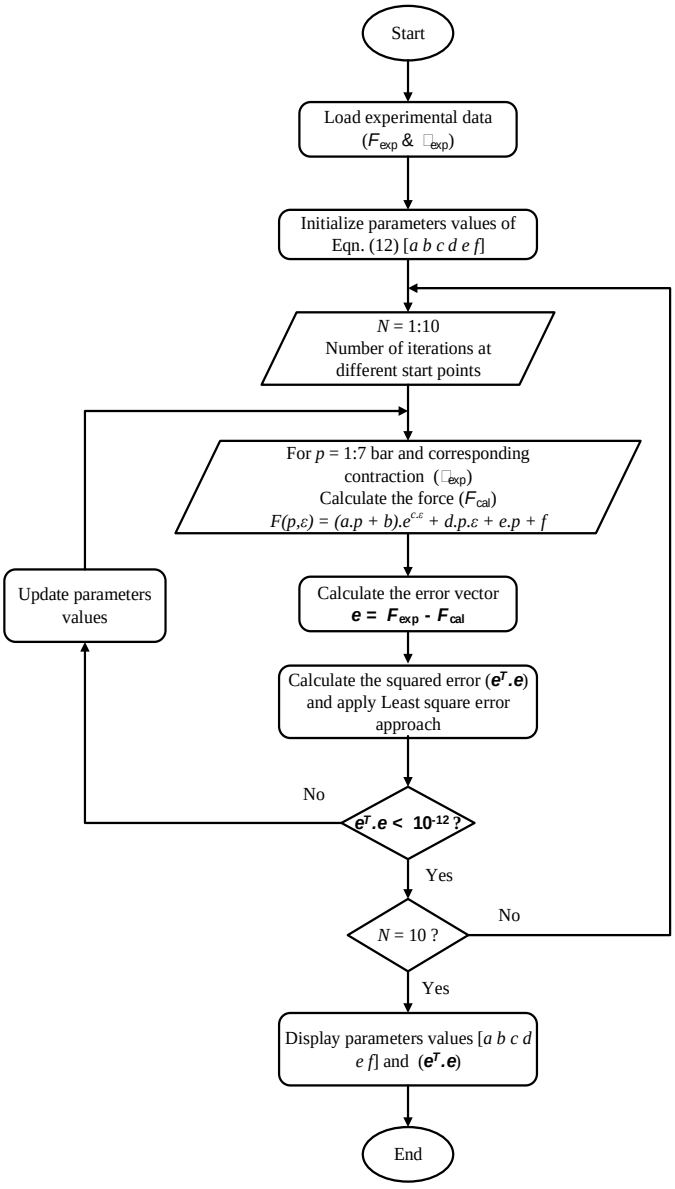

Fig. 7 Flowchart of the identification algorithm.

The algorithm procedures are given as follows:

- For each applied pressure (1-7 bar), the experimental results of the load (F_{exp}) and the corresponding contraction ($\mathcal{E}_{exp}$) is loaded and formulated by the vectors:

$$F_{exp} = \left[F_{1P_1} \dots F_{JP_1} \dots F_{1P_N} \dots F_{JP_N}\right]^T \quad (13)$$

$$\boldsymbol{\varepsilon_{exp}} = \left[\varepsilon_{1P_1} \dots \varepsilon_{JP_1} \dots \varepsilon_{1P_N} \dots \varepsilon_{JP_N}\right]^T \quad (14)$$

Where J = 1:13 represents the number of experimental points for each applied pressure and N = 1:7 denotes to the working pressure.

- Initialize the values of the model parameters as [a b c d e f] = [-9.219 203.701 -0.34221042 -3.226 109.203 -208.372] based on J. Sárosi and Z. Fabulya [32].
- For each measured contraction (ε_{JP_N}), the muscle force (F_{cal}) is calculated using Eqn. (12). After that the calculated muscle force vector ($\boldsymbol{F_{cal}}$) is for all measured contraction points with the same size of ($\boldsymbol{F_{exp}}$).
- Calculate the error vector between the experimental and calculated force vectors as:

$$\mathbf{e} = \mathbf{F_{exp}} - \mathbf{F_{cal}} \quad (15)$$

where $\boldsymbol{F_{exp}}$ and $\boldsymbol{F_{cal}}$ represent the experimental and calculated force vectors, respectively.

- Calculating the squared error vector:

$$\mathbf{e^T}.\mathbf{e} = \sum_{i=1}^{m} e_i^2 \quad (16)$$

where, e_i represents the error between the experimental and calculated forces for certain contraction and applied pressure, and m the number of experimental points, respectively.

- Optimizing the model parameters using the least square error approach.

The optimization options are set to 10^{-12} squared error and 10 times multi-start to ensure the optimized values of the parameters.

IV. RESULTS AND DISCUSSION

In this section, the results of the parameters identification of Eqns. (3), (4), (8), (9), and (12) are introduced. The identification results consider the range of the experimental data of the applied force, pressure, and the corresponding contraction. A correlation index based on the difference between the calculated force from the identified parameters and the experimental force is used as a metering index for evaluating the different models.

Referring to Fig. 5, it shows the PAM force upon applying different pressures with the corresponding contraction suggested by the muscle manufacturer. For a constant applied pressure, as the muscle load decreases, the corresponding

DOI: 10.21608/ERJENG.2023.179380.1131

Journal of Engineering Research (ERJ)
©Tanta University, Faculty of Engineering
https://erjeng.journals.ekb.eg/
ISSN: 2356-9441
e ISSN: 2735-4873

contraction is increasing and reaching its maximum at zero load. Fig. 8 shows the experimental results of the muscle force and the corresponding contraction at different applied pressures over the examined range (1:7 bar and 0:30 kg). From the two figures, clearly, the experimental results are in accordance with that of the manufacturer.

Figs. (9-a) and (10-a) show the results of the application of the identification algorithm on Eqn. (3). Fig. 9 presents the calculated force of the muscle at different applied pressures and the corresponding contraction compared to the experimental ones. The parameters of Eqn. (3), *b* and *n*, are obtained as 0.0099 and 8.9212, respectively. As it's clear from Fig. (9-a), Eqn. (3) is not well fitting the experimental results since the difference between the calculated muscle force and the experimental values for the same applied pressure and contraction is large. Fig. (10-a) shows the cross-correlation index for this approach. It has a value and a squared one as ($R = 0.8185$ and $R^2 = 0.6699$).

Figs. (9-b) and (10-b) show the identification results based on Eqn. (4). The parameter of Eqn. (4), θ, is obtained as 28.975°. Fig. (9-b) shows that Eqn. (4) also exhibits low fitting of the experimental results. Fig. (10-b) shows the calculated cross-correlation index for this approach given as ($R = 0.8667$ and $R^2 = 0.7512$).

Figs. (9-c) and (10-c) show the identification results based on Eqn. (8). The parameters of Eqn. (8), θ, a_k and b_k are obtained as 24.9921°, 3.55, and -2.1079, respectively. Fig. (9-c) shows better matching between the calculated forces and the measured ones at some applied pressures. However, the difference is still remarkable, especially at low pressures. Fig. (10-c) shows the calculated cross-correlation index for this approach given as ($R = 0.9267$and $R^2 = 0.8589$).

Figs. (9-d) and (10-d) show the identification results based on Eqn. (9). The parameters of Eqn. (9), θ, ak, bk, aε, and bε are obtained as 51.069°, 3.55, -0.372, 17.679, and -15.448, respectively. Fig. (9-d) exhibits an improvement in the trend of the fitting curves compared to the experimental results, but still, a noticeable difference exists between the calculated and experimental forces at low pressures. Fig. (10-d) shows the calculated cross-correlation index for this given as ($R = 0.9811$ and $R2 = 0.9267$).

Finally, Figs. (9-e) and (10-e) show the identification results based on Eqn. (12). As it appears from Fig. (9-e), good matching between the fitted data and the experimental one except at low load values for some applied pressures.

The parameters values of Eqn. (12), *a*, *b*, *c*, *d*, *e*, and *f* are obtained as -5.699, 158.773, -42.647, -299.482, 86.216, and -196.865, respectively. Fig. (10-e) shows the calculated cross-correlation index for this approach given as ($R = 0.9992$ and $R^2 = 0.9983$). Hence, the identification of the final approach exhibits the best results for the experimental data over the examined range of the applied pressures and loads.

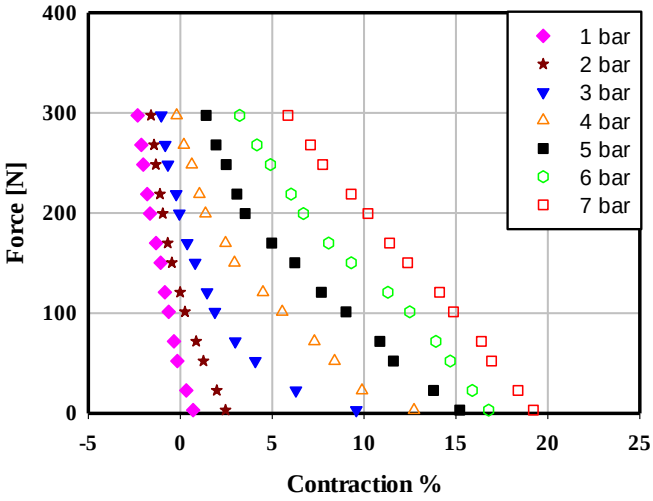

Fig. 8. Experimental Force against applied pressure and contraction.

V. CONCLUSION

This work highlights an accurate mathematical model for describing the performance of PAMs under different applied pressures and loads. Since the muscle is to be used to actuate a wrist rehabilitation robot, it's interested to figure out the suitable model for the muscle when operating at low applied forces. The experimental set-up involves a load range of 0:30kg and a gauge pressure range of 1:7bar. Then, an algorithm has been developed on MATLAB software based on the least square error approach to fit the experimental results based on previous work of five different identification approaches. The obtained conclusions can be listed as follows:

The first four approaches that are based on the geometrical characteristics of the muscle give poor fitting with the experimental results as given by their cross-correlation index values 0.8185, 0.8185 and 0.8667 for the first three approaches and 0.9267 for the fourth one which produces little enhancement.

The final approach, which is not based on the muscle geometrical characteristics, exhibits the best fitting over the examined range of the applied pressures and loads. It gives a correlation index of 0.9992.

As an extension of this work, the dynamic behavior of the muscle will be examined for the actuation in a wrist rehabilitation robot.

Funding: This research has not been conducted under any fund.

Conflicts of Interest: The authors declare that there is no conflict of interest.

DOI: 10.21608/ERJENG.2023.179380.1131

Journal of Engineering Research (ERJ)
©Tanta University, Faculty of Engineering
https://erjeng.journals.ekb.eg/
ISSN: 2356-9441
e ISSN: 2735-4873

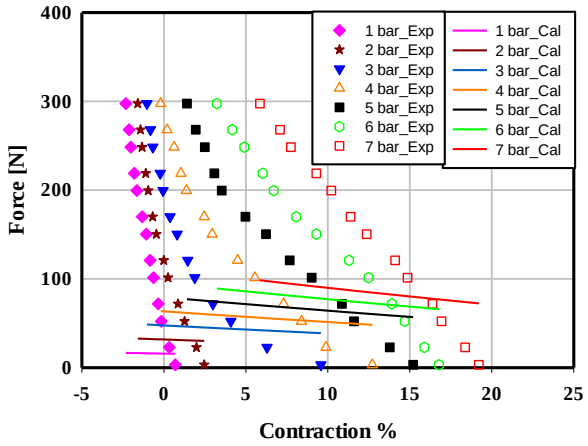

(a) Identification results of Eqn. (3)

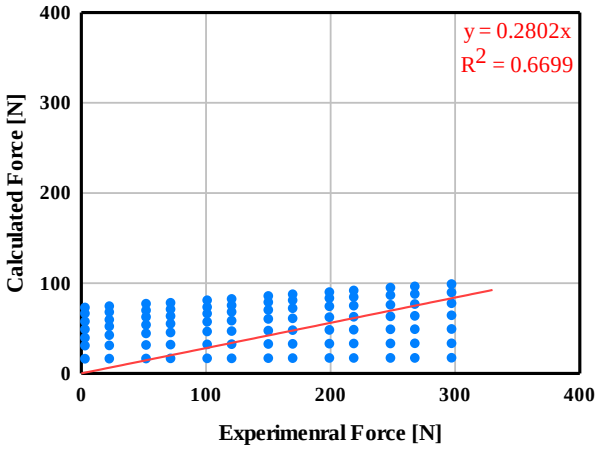

(a) Correlation index of Eqn. (3)

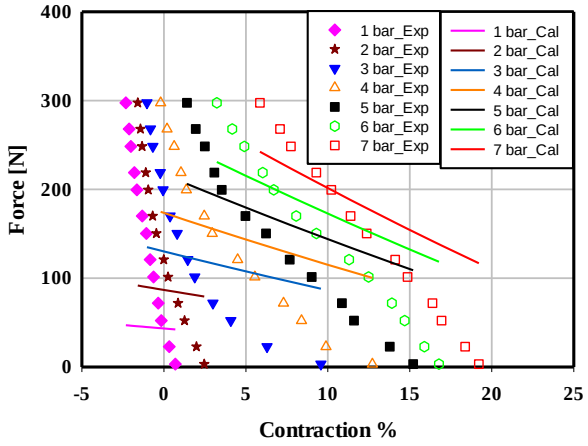

(b) Identification results of Eqn. (4)

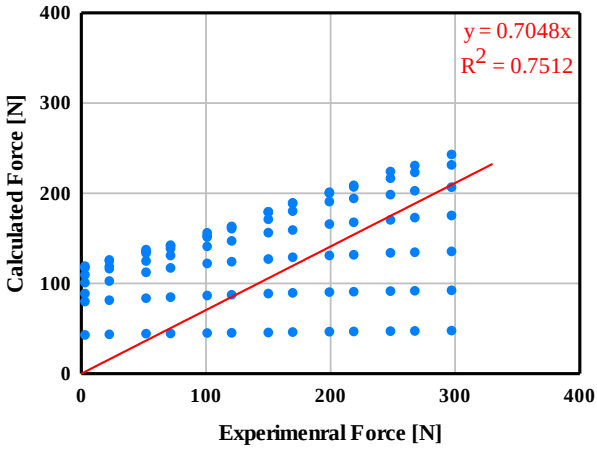

(b) Correlation index of Eqn. (4)

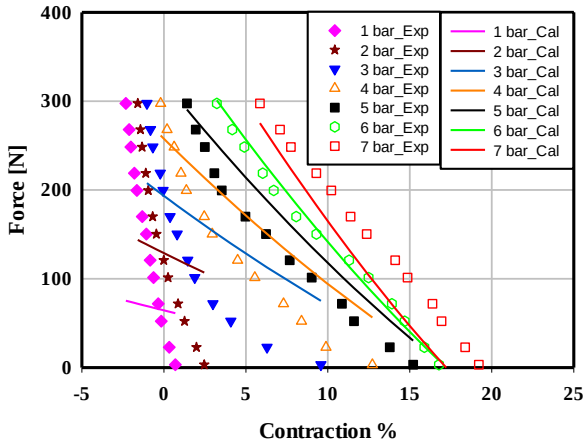

(c) Identification results of Eqn. (8)

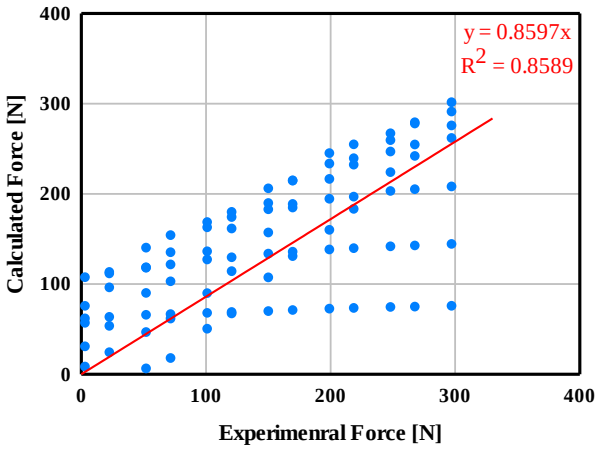

(c) Correlation index of Eqn. (8)

DOI: 10.21608/ERJENG.2023.179380.1131

Journal of Engineering Research (ERJ)
©Tanta University, Faculty of Engineering
https://erjeng.journals.ekb.eg/
ISSN: 2356-9441
e ISSN: 2735-4873

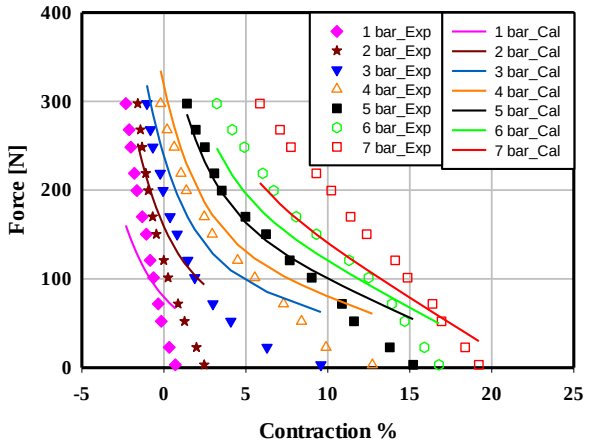

(d) Identification results of Eqn. (9)

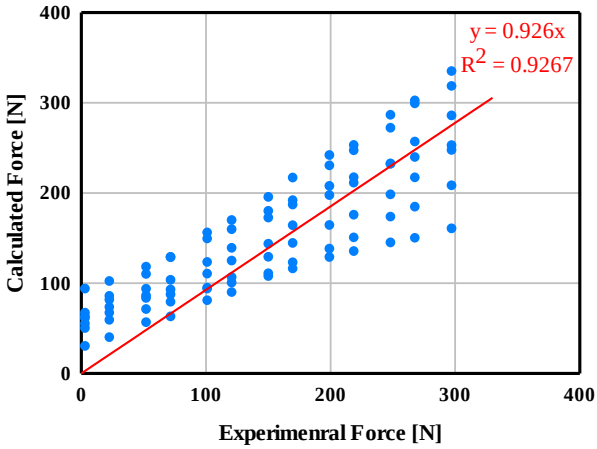

(d) Correlation index of Eqn. (9)

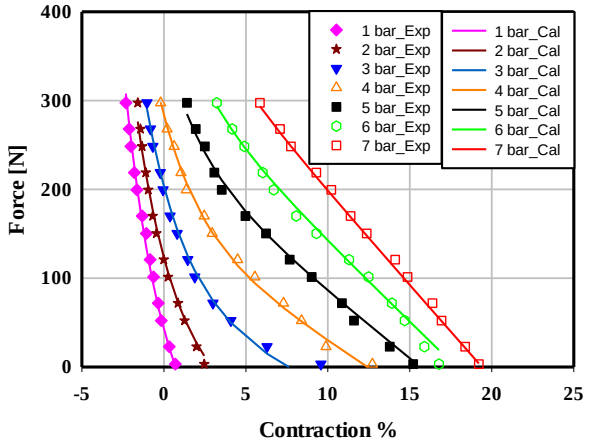

(e) Identification results of Eqn. (12)

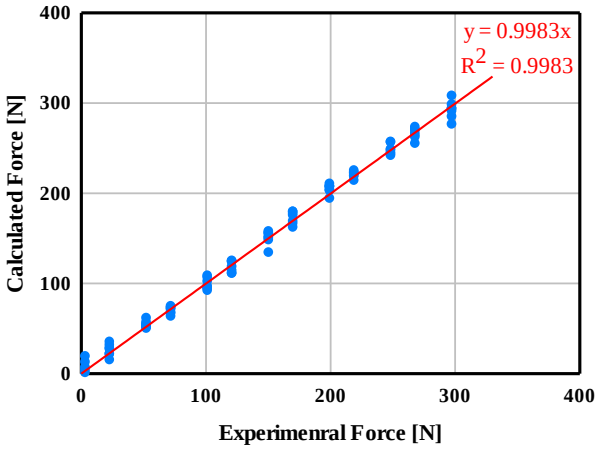

(e) Correlation index of Eqn. (12)

Fig. 9 Experimental and calculated results for different identification approaches.

Fig. 10 The correlation index for different identification approaches.

REFERENCES

[1] F. Daerden and D. Lefeber, "Pneumatic artificial muscles: actuators for robotics and automation," *European journal of mechanical and environmental engineering*, vol. 47, no. 1, pp. 11-21, 2002.

[2] M. D. Doumit and S. Pardoel, "Dynamic contraction behaviour of pneumatic artificial muscle," *Mechanical Systems and Signal Processing*, vol. 91, pp. 93-110, 2017.

[3] D. Caldwell, G. Medrano-Cerda, and M. Goodwin, "Braided pneumatic actuator control of a multi-jointed manipulator," in *Proceedings of IEEE Systems Man and Cybernetics Conference-SMC*, 1993, vol. 1, pp. 423-428: IEEE.

[4] V. L. Nickel, J. Perry, and A. L. Garrett, "Development of useful function in the severely paralyzed hand," *JBJS*, vol. 45, no. 5, pp. 933-952, 1963.

[5] H. Schulte, "The characteristics of the McKibben artificial muscle," *The application of external power in prosthetics and orthotics*, pp. 94-115, 1961.

[6] S. Laksanacharoen, "Artificial muscle construction using natural rubber latex in Thailand," in *The 3rd Thailand and material science and technology conference*, 2004, pp. 10-11.

[7] N. Takesue, J. Furusho, and Y. Kiyota, "Fast response MR-fluid actuator," *JSME International Journal Series C Mechanical Systems, Machine Elements and Manufacturing*, vol. 47, no. 3, pp. 783-791, 2004.

[8] D. Caldwell and N. Tsagarakis, "Biomimetic actuators in prosthetic and rehabilitation applications," *Technology and Health Care*, vol. 10, no. 2, pp. 107-120, 2002.

[9] F. Daerden, "Conception and realization of pleated artificial muscles and their use as compliant actuation elements," *PhD Dissertation*, pp. 5-33, 1999.

[10] K. Wickramatunge and T. Leephakpreeda, "Empirical modeling of pneumatic artificial muscle," in *Proceedings of the International MultiConference of Engineers and Computer Scientists*, 2009, vol. 2, no. 0: Citeseer Princeton, NJ, USA.

[11] G. Wszołek, G. Stawarz, and P. Zub, "The laboratory stand for didactic and research of a Fluidic Muscle," *Journal of*

DOI: 10.21608/ERJENG.2023.179380.1131

Journal of Engineering Research (ERJ)
©Tanta University, Faculty of Engineering
https://erjeng.journals.ekb.eg/
ISSN: 2356-9441
e ISSN: 2735-4873

Achievements in Materials and Manufacturing Engineering, vol. 25, no. 2, 2007.

[12] N. Wereley, C. Kothera, E. Bubert, B. Woods, M. Gentry, and R. Vocke, "Pneumatic artificial muscles for aerospace applications," in *50th AIAA/ASME/ASCE/AHS/ASC Structures, Structural Dynamics, and Materials Conference 17th AIAA/ASME/AHS Adaptive Structures Conference 11th AIAA No*, 2009, p. 2140.

[13] B. Hannaford and J. Winters, "Actuator properties and movement control: biological and technological models," in *Multiple muscle systems*: Springer, 1990, pp. 101-120.

[14] T. Noritsugu, M. Takaiwa, and D. Sasaki, "Development of power assist wear using pneumatic rubber artificial muscles," *Journal of Robotics and Mechatronics*, vol. 21, no. 5, p. 607, 2009.

[15] C. Vimieiro, B. G. do Nascimento, D. A. P. Nagem, and M. Pinotti, "Development of a hip orthosis using pneumatic artificial muscles," *Proceeding of TMSi, São Paulo, Spain*, pp. 18-19, 2005.

[16] M. Knestel, E. Hofer, S. K. Barillas, and R. Rupp, "The artificial muscle as an innovative actuator in rehabilitation robotics," *IFAC Proceedings Volumes*, vol. 41, no. 2, pp. 773-778, 2008.

[17] M. V. Damme, R. V. Ham, B. Vanderborght, F. Daerden, and D. Lefeber, "Design of a "soft" 2-DOF planar pneumatic manipulator," in *Climbing and Walking Robots*: Springer, 2006, pp. 559-566.

[18] D. A. Kingsley, R. D. Quinn, and R. E. Ritzmann, "A cockroach inspired robot with artificial muscles," in *2006 IEEE/RSJ International Conference on Intelligent Robots and Systems*, 2006, pp. 1837-1842: IEEE.

[19] P. Scarfe and E. Lindsay, "Air muscle actuated low cost humanoid hand," *International Journal of Advanced Robotic Systems*, vol. 3, no. 2, p. 22, 2006.

[20] B. Tondu and P. Lopez, "Modeling and control of McKibben artificial muscle robot actuators," *IEEE control systems Magazine*, vol. 20, no. 2, pp. 15-38, 2000.

[21] C.-P. Chou and B. Hannaford, "Measurement and modeling of McKibben pneumatic artificial muscles," *IEEE Transactions on robotics and automation*, vol. 12, no. 1, pp. 90-102, 1996.

[22] T. Szépe and J. Sárosi, "Matlab models for pneumatic artificial muscles," Scientific Bulletin of The Politechnica University of Timisoara Transactions on Mechanics, vol. 54, no. Special Issue 1, pp. 65-70, 2009.

[23] Y. Zhang, H. Liu, T. Ma, L. Hao, and Z. Li, "A comprehensive dynamic model for pneumatic artificial muscles considering different input frequencies and mechanical loads," *Mechanical Systems and Signal Processing*, vol. 148, p. 107133, 2021.

[24] I. M. Petre, "Studies regarding the Use of Pneumatic Muscles in Precise Positioning Systems," *Applied Sciences*, vol. 11, no. 21, p. 9855, 2021.

[25] F. F. Muscle, "with Press-fitted Connections, Fluidic Muscle MAS, with Screwed Connections," *Festo product catalogue*, 2005.

[26] F. Daerden, "Conception and realization of pleated pneumatic artificial muscles and their use as compliant actuation elements," *Vrije Universiteit Brussel*, p. 176, 1999.

[27] N. Tsagarakis and D. G. Caldwell, "Improved modelling and assessment of pneumatic muscle actuators," in *Proceedings 2000 ICRA. Millennium Conference. IEEE International Conference on Robotics and Automation. Symposia Proceedings (Cat. No. 00CH37065)*, 2000, vol. 4, pp. 3641-3646: IEEE.

[28] J. Albienz, R. Dillmann, T. Kerscher, and J. Zollner, "Dynamic Modelling of Fluidic Muscles using Quick-Release," ed: Forschungszentrum Informatik, Germany, 2005.

[29] J. Piteľ, "Modelling of the PAM based antagonistic actuator," *Cybernetic Letters*, 2008.

[30] J. Sárosi and Z. Fabulya, "New function approximation for the force generated by fluidic muscle," *Annals of the Faculty of Engineering Hunedoara*, vol. 10, no. 2, p. 105, 2012.

[31] J. Sárosi, Z. Fabulya, G. Keszthelyi-Szabó, and P. Szendrő, "Investigations of Precise Function Approximation for the Force of Fluidic Muscle in MS Excel," *ANALECTA TECHNICA SZEGEDINENSIA*, vol. 2012, no. CD Suppl., pp. CD-8 o., 2012.

[32] J. Sárosi and Z. Fabulya, "Mathematical analysis of the function approximation for the force generated by pneumatic artificial muscle," *Scientific Bulletin Of The Politechnica University Of Timisoara Transactions On Mechanics*, vol. 57, no. Special Issue 1, pp. 59-64, 2012.

DOI: 10.21608/ERJENG.2023.179380.1131